NASA/TM—2008-215279

Adsorption of Water on Simulated Moon Dust Samples

John P. Goering, Shweta Sah, and Uwe Burghaus
North Dakota State University, Fargo, North Dakota

Kenneth W. Street, Jr.
Glenn Research Center, Cleveland, Ohio

September 2008

NASA STI Program . . . in Profile

Since its founding, NASA has been dedicated to the advancement of aeronautics and space science. The NASA Scientific and Technical Information (STI) program plays a key part in helping NASA maintain this important role.

The NASA STI Program operates under the auspices of the Agency Chief Information Officer. It collects, organizes, provides for archiving, and disseminates NASA's STI. The NASA STI program provides access to the NASA Aeronautics and Space Database and its public interface, the NASA Technical Reports Server, thus providing one of the largest collections of aeronautical and space science STI in the world. Results are published in both non-NASA channels and by NASA in the NASA STI Report Series, which includes the following report types:

- TECHNICAL PUBLICATION. Reports of completed research or a major significant phase of research that present the results of NASA programs and include extensive data or theoretical analysis. Includes compilations of significant scientific and technical data and information deemed to be of continuing reference value. NASA counterpart of peer-reviewed formal professional papers but has less stringent limitations on manuscript length and extent of graphic presentations.

- TECHNICAL MEMORANDUM. Scientific and technical findings that are preliminary or of specialized interest, e.g., quick release reports, working papers, and bibliographies that contain minimal annotation. Does not contain extensive analysis.

- CONTRACTOR REPORT. Scientific and technical findings by NASA-sponsored contractors and grantees.

- CONFERENCE PUBLICATION. Collected papers from scientific and technical conferences, symposia, seminars, or other meetings sponsored or cosponsored by NASA.

- SPECIAL PUBLICATION. Scientific, technical, or historical information from NASA programs, projects, and missions, often concerned with subjects having substantial public interest.

- TECHNICAL TRANSLATION. English-language translations of foreign scientific and technical material pertinent to NASA's mission.

Specialized services also include creating custom thesauri, building customized databases, organizing and publishing research results.

For more information about the NASA STI program, see the following:

- Access the NASA STI program home page at *http://www.sti.nasa.gov*

- E-mail your question via the Internet to *help@sti.nasa.gov*

- Fax your question to the NASA STI Help Desk at 301–621–0134

- Telephone the NASA STI Help Desk at 301–621–0390

- Write to:
  NASA Center for AeroSpace Information (CASI)
  7115 Standard Drive
  Hanover, MD 21076–1320

NASA/TM—2008-215279

Adsorption of Water on Simulated Moon Dust Samples

John P. Goering, Shweta Sah, and Uwe Burghaus
North Dakota State University, Fargo, North Dakota

Kenneth W. Street, Jr.
Glenn Research Center, Cleveland, Ohio

National Aeronautics and
Space Administration

Glenn Research Center
Cleveland, Ohio 44135

September 2008

Acknowledgments

Level of Review: This material has been technically reviewed by technical management.

Available from

Adsorption of Water on Simulated Moon Dust Samples

John P. Goering, Shweta Sah, and Uwe Burghaus
North Dakota State University
Fargo, North Dakota 58105

Kenneth W. Street, Jr.
National Aeronautics and Space Administration
Glenn Research Center
Cleveland, Ohio 44135

Abstract

A lunar regolith simulant dust sample (JSC-1a) supported on a silica wafer (SiO_2/Si(111)) has been characterized by scanning electron microscopy (SEM), energy dispersive x-ray spectroscopy (EDX), and Auger electron spectroscopy (AES). The adsorption kinetics of water has been studied primarily by thermal desorption spectroscopy (TDS) and also by collecting isothermal adsorption transients. The support has been characterized by water TDS. JSC-1a consists mostly of aluminosilicate glass and other minerals containing Fe, Na, Ca, and Mg. The particle sizes span the range from a few microns up to 100 μm. At small exposures, H_2O TDS is characterized by broad (100 to 450 K) structures; at large exposures distinct TDS peaks emerge that are assigned to amorphous solid water (145 K) and crystalline ice (165 K). Water dissociates on JSC-1a at small exposures but not on the bare silica support. It appears that rather porous condensed ice layers form at large exposures. At thermal impact energies, the initial adsorption probability amounts to 0.92±0.05.

Introduction

Motivation

Remote sensing probes sent to the Moon in the late 1990s (refs. 1 to 3) signaled that water may exist on the Moon buried under lunar regolith (surface rocks and dust), in areas such as the bottom of deep, permanently shadowed craters at the lunar poles. Water is of paramount importance for any exploration and colonization project that would require self-sustainable systems on the Moon. Therefore, investigating the interaction of water with lunar regolith, using all terrestrial techniques, is pertinent to future exploration. The lunar environment can be approximated in an ultra-high vacuum (UHV) system. In addition, water that covers most solid surfaces is the most abundant compound on Earth and its interaction with surfaces is pertinent for a variety of diverse disciplines including catalysis, corrosion, solar energy conversion (ref. 4), geochemistry (e.g., atmospheric degradation due to the effect of water vapor) (refs. 5 and 6), meteorology, and design of lunar equipment (ref. 7). Furthermore, chemical reactions on ice surfaces (clouds) in the stratosphere can affect the ozone balance on Earth (ref. 8).

Lunar regolith specimens collected during the Apollo missions in the 1970s are still available (ref. 9). However, extensive testing of simulated lunar regolith material is required before any application for real lunar samples can be justified. For this reason, a number of simulated lunar regolith materials have been developed for NASA Marshall Space Flight Center (MSFC). The sample used here (JSC-1a) consists mostly of aluminosilicate glass and minerals, which contain Fe, Na, Ca, and Mg with particle sizes of the raw material up to 1000 μm. The JSC-1a is further classified as a lunar mare simulant containing basaltic material high in glass content (~50 percent) having substantial amounts of plagioclase (37 percent) and lesser amounts of minerals such as olivine (9 percent) with traces of a number of other minerals (<1 percent each) (ref. 10). These findings have been confirmed by XRD (x-ray diffraction) studies indicating the presence of substantial crystalline material (ref. 11).

The objectives of this project were

(1) Manufacturing of samples (based on JSC-1a powder) that allow for using analytical surface chemistry and kinetics tools using as little raw "lunar" materials as possible. For example, are the van der Waals forces of the simulant crystallites large enough to apply the drop-and-dry technique developed in studies of nanomaterials (ref. 12)? If this approach is successful, then it could be applied to other materials in order to directly study, for example, powder catalysts bridging the materials gap.

(2) Evaluating the possible application of electron probe techniques such as Auger electron spectroscopy (AES) to the study of these samples. How large are charging effects of the sample?

(3) Characterizing the adsorption kinetics of water on the lunar regolith dust simulant. This has implications on the probability of finding water on the Moon and, if present, on recovery techniques used to harvest it for human sustainability.

Related Surface Chemistry Literature

Water is likely the most often studied probe molecule in surface science, frequently leading to very complicated overlayer structures and kinetics as reviewed in references 13 to 15. Questions about whether water dissociates, how efficiently it wets different surfaces, the degree of crystallization, details of the water-ice transition, and cluster formation kinetics remain subjects of controversy. The bilayer model proposed in the 1980s assumes molecular water adsorption in the monolayer coverage range and formation of bilayers of water molecules hydrogen bonded to the monolayer prior to the condensation of ice multilayers. At very low adsorption temperatures (<100 K) water monomers may be present, which cluster at greater temperatures (100 to 140 K) forming amorphous solid water (ASW). At even greater temperatures, crystalline ice (CI) is formed (at UHV conditions above 140 to 150 K with cubic structure and at ~200 K hexagonal CI can form) via a phase transition involving viscous water (glass transition at ~135 K) (ref. 16). Complex thermal desorption spectroscopy (TDS) data consisting of multiple features have been obtained for condensed water films and are related to subtle rearrangements of the water adlayer, which are still debated even for one-component single-crystal systems (refs. 13 and 14). It has been argued that the amorphous to crystalline ice transition is independent of the substrate (ref. 14); that is, the phase nucleation occurs within the ice film. Therefore, it is of interest to study a highly disordered system where the micron particles may act as nucleation sites. Distinct differences of water adsorption and/or desorption from steps and terrace sites of single-crystal surfaces has been reported, with water found to preferentially adsorb along steps (ref. 17).

Although water adsorption on largely inhomogeneous multicomponent systems such as steel (ref. 18) or $Bi_2Sr_2CaCuO_8$ (high-temperature superconductor) (ref. 5) have been studied in vacuum by kinetic techniques, we are not aware of UHV surface science studies about water adsorption on aluminosilicates. Therefore, systems containing O, Si, Al, Ca, Mg, and Fe (the main components of JSC-1a) may be the best reference systems currently available. We restrict this very brief literature survey to a number of kinetics experiments.

Oxides that are terminated by reactive metal surface atoms tend to dissociate water, whereas oxide surfaces that are terminated by oxygen are more inert (ref. 19). For FeO(111) films, water adsorbs molecularly with well-resolved monolayer and multilayer TDS peaks. Above adsorption temperatures of 120 K, ordered two-dimensional islands form that completely cover (wet) the surface at saturation (ref. 20). In contrast, water dissociates on $Fe_3O_3(111)$, which exposes Fe sites (ref. 19). Similarly, dissociation of water is reported for the Al-terminated $Al_2O_3(0001)$ surface, but not for O-terminated sapphire films (see ref. 19 and references therein). However, water adsorption even on defect-free MgO thin films leads to dissociation and hydroxyl formation (ref. 21). According to recent results, no dissociation of water is seen for defect-free SiO_2 thin films, nor are extended defects on SiO_2 surfaces (refs. 22 and 23). However, oxygen vacancy sites on some metal oxides can lead to water dissociation (ref. 24). The interaction of condensed water with hydroxyl groups or oxygen yields complex TDS curves (ref. 25). In addition, CaO surfaces (Ca is a major component of JSC-1a), which expose Ca- and O-sites,

are catalytically very active towards dissociative water adsorption (ref. 26), and powders of CaO appear to be efficiently hydroxylated (ref. 13).

Related Studies on Lunar Dust Samples and Implications for NASA Applications

We are aware of a few early studies that applied surface science techniques to lunar samples (see ref. 27 photoemission spectroscopy). To the best of our knowledge, no kinetics studies with water have been conducted at UHV conditions with surface science tools. However, a number of studies in the 1970s have been conducted on powder specimens, including measurements of adsorption isotherms at high-vacuum conditions (ref. 28). Recently the effect of water on mineral degradation has been considered comparing lunar, Martian, and Earth environments (refs. 6, 29, and 30). Mineral degradation is important in designing lunar equipment to handle abrasive wear, while degraded terrestrial mineral simulants may underestimate the damage caused by lunar counterparts. Scanning electron microscopy (SEM) characterization of this material reveals the pointed nature of the fractured particles. Because the JSC-1a components have moderate hardness, the pointed particles will be abrasive to construction materials useful for lunar exploration including polymers, some glasses, and many metals. Terrestrial minerals lose hardness with surface water adsorption (see ref. 6 and references therein); therefore, their lunar counterparts will be harder. This is important to designers of lunar exploration equipment since the abrasive nature of the minerals are directly related to the ratio of the hardness of the mineral to the construction material; as this ratio approaches 1.0, the mineral will become abrasive and will reach maximum and nearly constant abrasiveness at a ratio of approximately 1.3. Minerals having high angularity will have higher abrasive qualities. Therefore, a study of the ability of these minerals to uptake water and lose surface hardness also has implications to design criteria.

Considering what is known from prior studies, dissociative adsorption (due to the high defect density and metal sites on the surface of the dust crystallites), as well as distinct clustering of water (due to the large defect density), may be expected for the JSC-1a system studied.

The JSC-1a powder supported on a silica wafer has been characterized by SEM, energy dispersive x-ray (EDX) fluorescence, and AES. The adsorption kinetics of water has been studied by TDS. In addition, the support has been characterized in order to distinguish support and JSC-1a effects.

Experimental Procedures

Surface chemistry measurements conducted at North Dakota State University used two standard UHV systems including a shielded mass spectrometer for TDS and a combined LEED (low energy electron diffraction) retarding field AES system available in one of the systems (ref. 31). Deionized water was dosed by backfilling the UHV chamber after several freeze-pump-thaw cycles. The reading of the thermocouple was calibrated ($\pm$5 K) in situ by TDS measurements of condensed alkanes. A background has been removed from the TDS curves; the heating rate amounts to 2 K/s. The exposures are given in Langmuir (1 L = 1 s gas exposure at 1×10^{-6} mbar).

Images were acquired on a Jeol JSM 840A SEM (Jeol Ltd.) equipped with an Edax Phoenix (Ametek, Inc.) to acquire the XRF spectra at NASA Glenn Research Center (GRC). The SEM images were run at 5 to10 kV in order to prevent charging of the nonconductive sample. After TDS experiments, the sample was lightly coated with Au, and SEM were acquired at 20 kV for a postcharacterization of the sample.

A silica wafer (from MEMS and Nanotechnology Exchange) specified as a 300-nm-thick SiO_2 layer on n-type Si(111) (bluish color and 1 to 10 Ωcm) was used as a support (ref. 32). The support was cleaned with acetone and methanol before depositing the JSC-1a powder. The powder was sieved with a 20-μm mesh. One micro spatula tip of this material was added to isopropanol and the suspension was sonicated with a bench top sonicator. Three 50-μL aliquots of the suspension were dropped-and-dried on the support resulting in a closed layer of simulated lunar regolith dust on the support, as judged by eye. The supported sample was degassed in UHV (annealing temperatures of up to 550 K have been used).

Presentation and Discussion of the Results

Sample Characterization

SEM

Figure 1 depicts SEM results of the JSC-1a dust simulant sample supported on a silica wafer obtained before (figs. 1(a) and (b)) and after the kinetics experiments (figs. 1(c) and (d)). The magnification factor and a scale bar are added to the figure. The SEM obtained after the UHV experiments have a better contrast since the samples have been covered with a Au film.[1]

The SEM results show that the van der Waals forces even of particles of a few microns up to 100 μm are large enough to anchor the stimulant on the support; the samples were stable and led to well-reproducible kinetics data for several weeks in the UHV chamber. Thus, the drop-and-dry technique, which requires only very small amounts of the raw material (<1 mg), can be applied to support even rather large particles on standard supports such as silica. According to the SEM results (fig. 1(c)), approximately 90 percent of the support was covered with the dust particles. Comparing SEM data collected before and after the UHV experiments (figs. 1(b) and (d)) indicates no sintering effects.
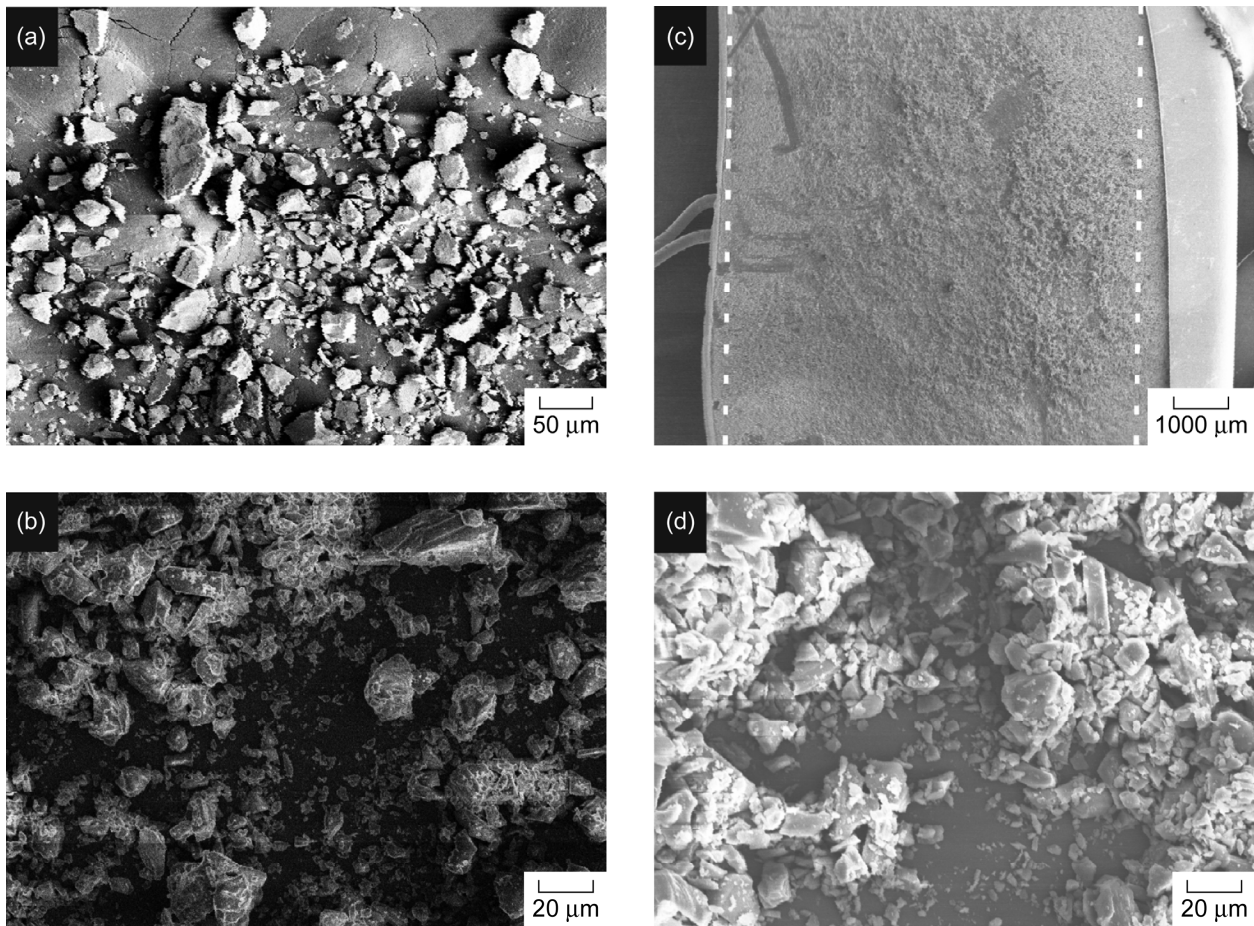

Figure 1.—Scanning electron microscopy (SEM) figures of the JSC-1a dust sample on a silica support collected (a) and (b) before and (c) and (d) after the ultra-high vacuum (UHV) experiments.

---

[1]At the rim of the low-magnification SEM (fig. 1(c)) parts of the sample holder are displayed. The silica wafer is within the dotted lines added to this figure.

EDX Spectroscopy

According to EDX spectra of the supported particles (averaged over the entire frame shown in figure 1(b) collected before the kinetics experiments), the JSC-1a consists of 34 percent Al, 25 percent Mg, 21 percent Ca, 14 percent Fe, and 5 percent Na as scaled with respect to the total signal of those components. Large silicon and oxygen signals were present in the EDX which cannot be separated from the support. EDX data collected after finishing the kinetics experiments gave the following composition of the sample: 49 percent Al, 16 percent Mg, 27 percent Ca, 3 percent Fe, and 4 percent Na. Thus, a 15 percent variation in the sample composition has been determined by the two spots examined with EDX, which most likely reflects the inhomogeneity of the sample.

The EDX spectra are typical of an aluminosilicate since the simulant was derived from volcanic ash of basaltic composition (San Francisco volcanic range, Flagstaff, AZ) (ref. 10). In an XRD study performed at GRC (ref. 11), the anorthositic nature of this mineral was confirmed in addition to the high glass content. Other unpublished spectroscopic investigations on a large number of particles revealed little variation in the composition between glass and mineral (refs. 10 and 11).

AES

AES identified Al, Ca, O, and Fe components of JSC-1a. The energetically low-lying Al and Mg AES signals, because of the secondary electron background, are difficult to detect with a retarding field AES system. Although, charging effects of the sample were present (~10 V peak shifts), AES could be applied, even using a standard support such as silica. No LEED pattern could be obtained either from the JSC-1a sample or thick water layers, as expected.

Adsorption of Water

Water Adsorption Kinetics on the Silica Support

TDS data of water adsorbed on the bare silica support at ~90 K are shown in figures 2(a) and (b), as a function of water exposure, $\chi(L)$.[2] At low exposures (fig. 3a), a rather symmetric structure (clustered water (CW) peak) is detectable at ~190 K, approximately independent of exposure that is consistent with first-order adsorption and desorption kinetics. No further TDS peaks are detectable up to temperatures of 500 K (fig. 2(c)); that is, no indications for H_2O dissociation are present for the silica support, in agreement with studies on silica thin films (ref. 22). The CW peak is clearly related with H_2O adsorption in the monolayer coverage range presumably to the formation of two-dimensional clusters (CW). Increasing the water exposure leads to a TDS structure emerging at ~150 K (ASW peak, fig. 2(b)). The leading edges of these peaks lineup indicating zeroth-order kinetics and formation of a condensed layer of ASW. The clear separation of the CW and ASW peaks allows for a coverage estimate by integrating the TDS curves. One monolayer has been assigned to the TDS curve at the onset of the ASW peak. A monolayer is defined as the amount of water required to form an icelike bilayer on the surface indicated by the appearance of the ASW TDS structure (ref. 33). An exposure of 0.6 to 1.0 L is required to saturate the monolayer; that is, the initial adsorption probability will be close to one, as expected. The largest exposures used correspond to ~100 monolayer. A minor shoulder present at large exposures may indicate the formation of CI (CI peak in fig. 2(b)).

Water Adsorption on the Supported Lunar Regolith Simulant Dust Sample

TDS data of water adsorbed at 100 K on the silica-supported JSC-1a dust sample are shown in figure 3. Figures 3(a) to (c) correspond to an increase in water exposure from 0.01 to 12 L, as indicated.

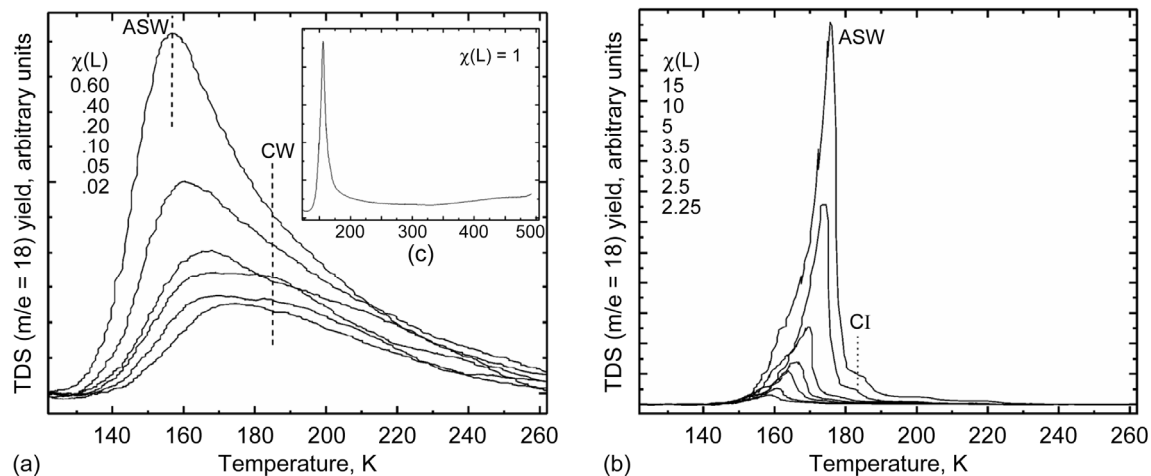[2]We recall that the surface of the support consists of a silica film on top of a silicon wafer.

Figure 2.—Thermal desorption spectroscopy (TDS) data of water adsorbed at 90 K on a bare silica wafer. (a) for small (t). (b) for large exposures, as indicated. (c) shows a TDS curve on an expanded scale.
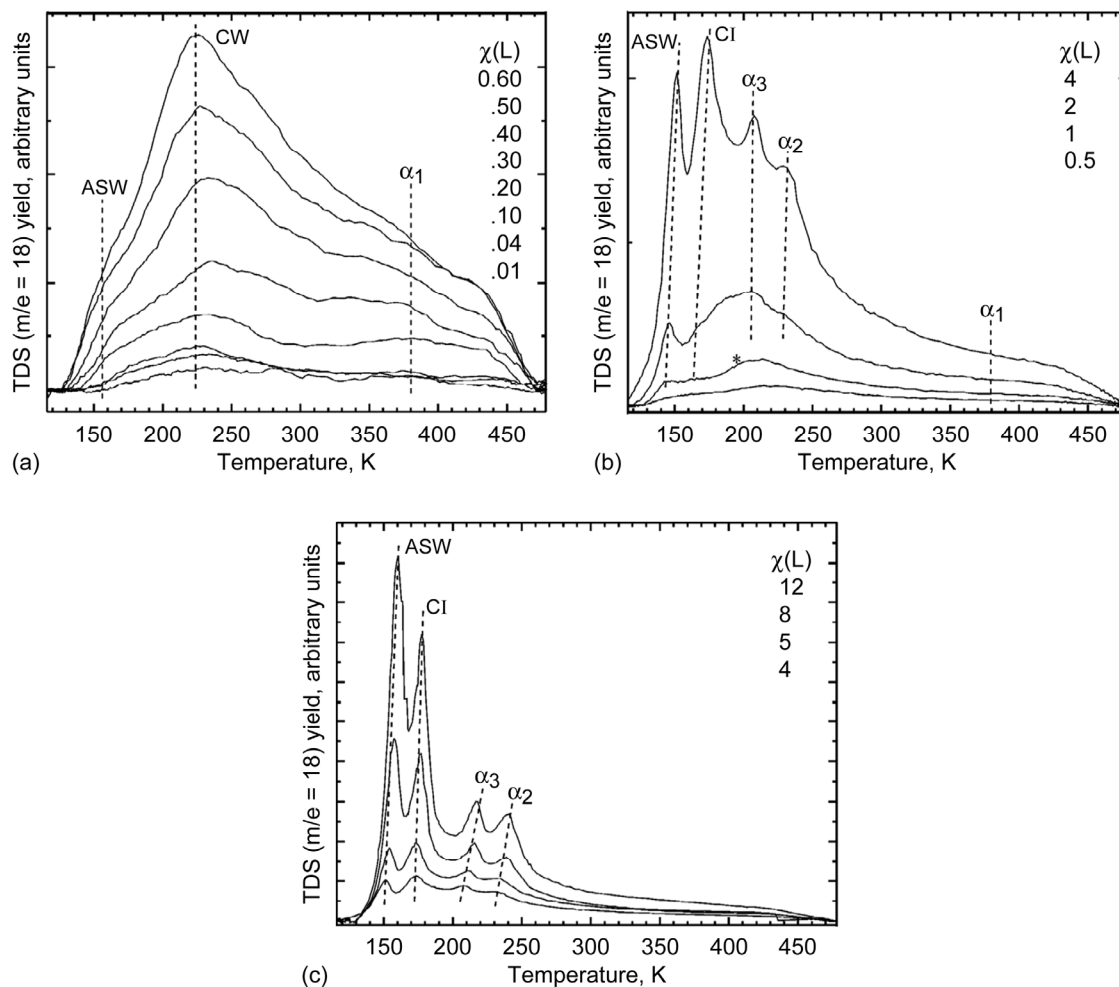

Figure 3.—Thermal desorption spectroscopy (TDS) of water from the JSC-1a dust sample supported on silica. The different panels show data obtained for different exposure regimes from (a) very small to (c) large exposures. Adsorption temperatures, T_{ads}, amounts to 90 K (amorphous solid water (ASW), crystalline ice (CI), α_3–α_2; OH-H_2O cluster; clustered water (CW) (monolayer range); α_1: recombinative desorption of water—see discussion).

Low exposure range.—At small exposures (fig. 3(a)) the TDS curves are dominated by a broad structure at 220 K, a large shoulder at about 380 K (α_1 peak), and an onset of another shoulder at ~150 K.

Comparing these data with the silica reference curves (fig. 2) suggests assigning the low-temperature shoulder (see fig. 3(a)) to the onset of the ASW peak (fig. 3(b)). The intensities of this shoulder peak are too small for assigning it to water adsorption on the JSC-1a dust particles. The ASW structure is readily observed at exposures as low as 0.1 L (fig. 3(a)), which indicates the formation of three-dimensional water clusters on the simulant sample as perhaps expected from scanning tunneling microscopy studies on stepped surfaces where the step edges could be identified as nucleation sites (ref. 17). Thus, the JSC-1a dust particles act as nucleation sites, which may result in a rather porous water film. This conclusion is further supported by coadsorption experiments.

The broad structure at 220 K is assigned to water adsorption in the monolayer coverage range on clean silica patches and JSC-1a particles. Note that according to the SEM estimate, the support is very well covered by the dust simulant in the probe area. Furthermore, the larger total surface area of the dust particles, as compared with the bare silica support, suggest that this structure is dominated by the effect of the simulant. The TDS peaks are labeled accordingly as CW and ASW. The CW peak on the bare silica support had a width of about 50 K (at 0.6 L) and the corresponding structure for JSC-1a/silica is significantly broader (at least 100 K at 0.6 L). This suggests either coverage dependent kinetics and/or kinetically distinct adsorption sites on the inhomogeneous sample.

Interestingly, a distinct structure that is not present for the bare silica support is the high-temperature α_1 peak (compare fig. 2(c) and fig. 3(a)). Therefore, we assign the high temperature α_1 TDS feature clearly to the effect of the JSC-1a particles. The great desorption temperature of this α_1 TDS peak suggests dissociative adsorption of water and recombinative desorption via adsorbed hydroxyls according to: $OH_{ads} + OH_{ads} \rightarrow H_2O_{gas} + O_{ads}$. Thus, the micron-sized particles catalyze H_2O dissociation.

Large exposure range.—At larger exposures (fig. 3(b)), three more TDS features emerge labeled as CI (onset at 165 K), α_3 (205 K), and α_2 (229 K). The CI peak can simply be identified as crystalline ice; similar TDS features have often been reported (refs. 13 and 14). For example, the CI TDS peak has been detected at 168 K (ref. 34) for Pt(111) and at 161 K for FeO(111) (ref. 20). Readsorption as the origin of the α_3 and α_2 peaks appears unlikely since these structures were (at similarly large exposures) not present on the bare silica support. Therefore, the α_3 and α_2 peaks are tentatively assigned to the formation of OH-H_2O clusters. The interaction of oxygen, hydroxyls, and water has been studied in great detail for metal surfaces and often leads to complicated multipeak TDS curves (refs. 13 and 14), for example, for Ag(111) OH-H_2O cluster-induced TDS, peaks have been detected at 225 K (ref. 25). Diffusion of OH through thick ice layers has been proposed (ref. 25). Increasing the exposure further, figure 3(c) clearly shows that the leading edges of the ASW peaks lineup, consistent with zeroth-order kinetics and condensed water films. In addition, also the low-temperature edges of the CI peaks appear to line up, as perhaps expected.

A variation of the adsorption temperature (from 104 to 174 K), while keeping the exposure constant (5 L), did not change significantly the position of the ASW, CW, α_3-α_1 TDS peaks (data not explicitly shown). However, the TDS features were quenched according to their order of binding strength. At an adsorption temperature of 174 K, only the α_2 and α_1 peaks remained detectable, as expected.

In order to estimate the coverage (number of porous ice layers) we assign the TDS curve where the ASW peak is clearly seen (at 1 L) to an apparent coverage of 1 monolayer (labeled by an asterisk in figure 3(b)). Accordingly, exposures of 4 and 12 L correspond to ~6 and ~50 monolayers, respectively.

Adsorption Dynamics of Water

Adsorption transients of water collected slightly above the condensation temperature have been obtained by the King and Wells technique by opening a leak valve fast (bulb experiments, ref. 35) in order to determine the adsorption probabilities more accurately. As expected (ref. 15), the initial adsorption probabilities, S_0, are close to one ($S_0 = 0.92 \pm 0.05$) consistent with the TDS data indicating the
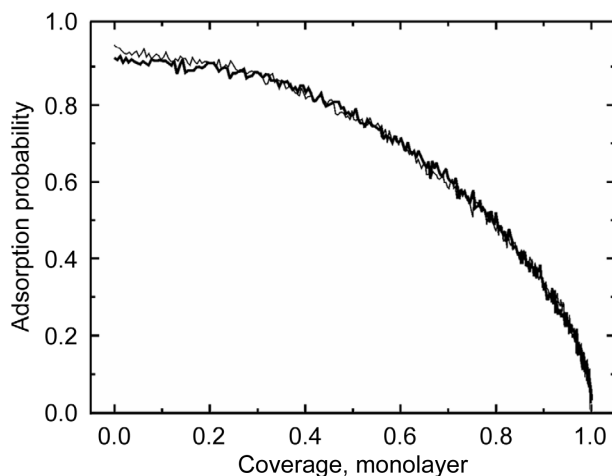
Figure 4.—Integrated adsorption isotherm
(adsorption probability versus coverage)
obtained by backfilling water at 153 K on
the JCS-1a dust sample (1×10^{-9} mbar,
T_{ads} = 153 K). Two curves obtained at
identical measuring conditions are depicted.

formation of a clear multilayer structure for exposures of roughly 1 L. The coverage dependence of the adsorption probability, $S(\Theta)$, obeys the typical Kisliuk shape (fig. 4). Thus, $S(\Theta)$ depends only weakly on coverage, Θ, up to saturation, as expected.

Water and Alkane Coadsorption

The coadsorption of water with inert molecules has been applied to gain information about the growth morphology of the ice layers (refs. 16, 20, and 36). Because of experimental constraints, coadsorption experiments with inert gases are currently not possible. Therefore, we used nonpolar n-pentane to collect coadsorption data with water; liquid alkanes and water are immiscible.

Reference data, where only n-pentane has been dosed on the stimulant, are shown in figures 5(a) and (b). We assign the broad features detectable already at small exposures and consisting of two overlapping structures, to n-pentane adsorption in the monolayer range. Experiments on clean silica wafer (see refs. 32 and 37) indicate that the high-temperature TDS feature is related with the bare silica (Si peak) and the lower temperature peak with adsorption of n-pentane on JSC-1a particles (JSC peak). The low-temperature peaks, with lined-up leading edges, are the signature of n-pentane condensation (C peak).

Figure 5(c) depicts TDS data. First a given amount of water (from 0 to 90 L as indicated) and afterwards a constant exposure of n-pentane (33 L) have been dosed on the JSC-1a sample. As evident, the n-pentane TDS feature at 165 K (fig. 5(c)) corresponds to n-pentane in the monolayer range (fig. 5(a)). The C peak corresponds to desorption of condensed n-pentane. Interestingly, the position of the monolayer TDS feature is independent of the water coexposure and roughly agrees with the data obtained for the clean silica support. These results would be consistent with the formation of a rather porous three-dimensional water layer allowing for diffusion of the alkane through the ice film. The large width of the TDS curves for n-pentane desorption from thick water layers (90 L water correspond to >100 monolayer) also indicates a large inhomogeneity of the frozen water film. The intensity of the condensation peak increases with water exposure and the intensity of the monolayer structure decreases, conserving the total area of the TDS peaks. Thus, clearly water and pentane compete about identical adsorption sites (ref. 38). In contrast, adsorption of pentane on a closed ice film should lead to a shift of the TDS peaks and different peak shapes as compared with the clean silica support (refs. 16 and 39).
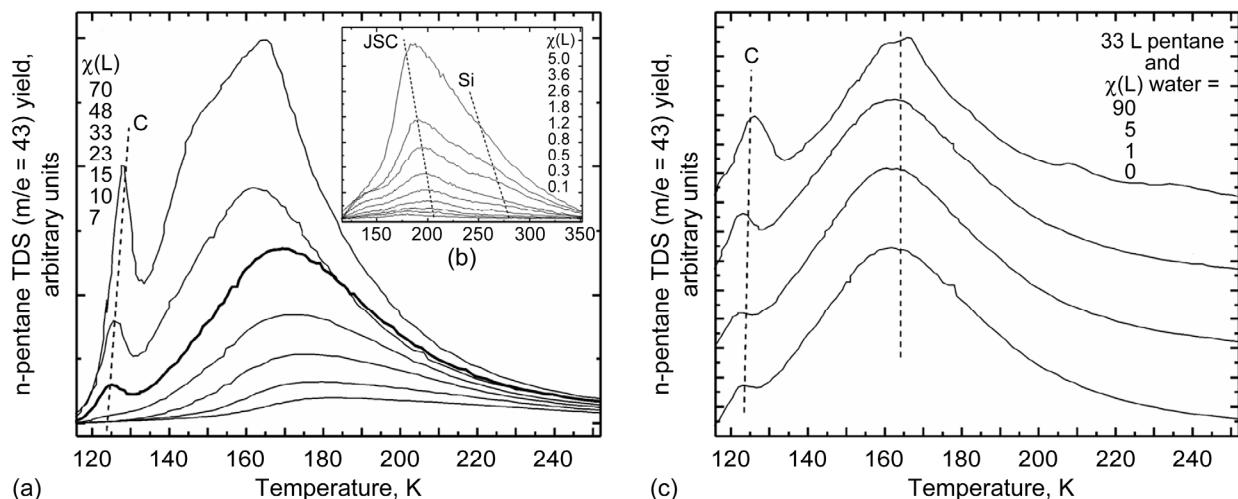
Figure 5.—(a) and (b) n-pentane thermal desorption spectroscopy (TDS) data obtained for the JSC-1a at large and small (inset) exposures. (c) Co-adsorption of n-pentane and water on JSC-1a/silica. The pentane exposure has been kept constant (33 L) and the water exposure varied, as indicated (T_{ads} = 90 K).

A diffusion of the nonpolar pentane through a thick and homogeneous ice layer appears unlikely. Therefore, we conclude the formation of rather porous ice films on the JSC-1a sample in agreement with the ASW TDS peak seen already at very small exposures (fig. 3(a)). Water does not wet the highly defected surface efficiently. Reversing the adsorption order (first pentane, then water) does not change significantly the shape and position of the TDS peaks. Attempts to observe a long-range order of thick water films by LEED failed. Both results are in agreement with the formation of rather porous films. Note that the transport of CO and chloroform through closed water films adsorbed on Pt(111) was efficiently blocked within a similar adsorption temperature range studies here (ref. 39). In addition, OH coadsorbed with water resulted in nonwetting behavior; large three-dimensional water clusters rather than continuous ice multilayer films are formed (ref. 39). As described above indications for dissociative water adsorption and adsorbed OH is present on the supported lunar regolith simulant.

Summary

The following information has been gathered:

1. Irrespective of the rather large particle sizes of the powder sample (<20 μm), the drop-and-dry technique could be applied successfully. Samples stable enough to apply sample temperature ramping techniques have been obtained.
2. The same methodology could be applied to catalyst powders in order to bridge the structure gap.
3. No indication for particle sintering has been obtained by SEM.
4. The chemical composition of JSC-1a could be analyzed by EDX and AES. The charging of the JSC-1a particles, even on a silica support, was not a bottleneck. Thus, AES can be applied to this type of sample.
5. A clear separation of monolayer and multilayer water TDS peaks was seen for the bare silica support.
6. Water dissociates on JSC-1a at low exposures, with TDS features detected at desorption temperatures as great as 450 K, which were not present for the bare support.
7. TDS data and coadsorption experiments provide some indications for the formation of three-dimensional water clusters on JSC-1a and a rather porous condensed water film. It appears plausible that the micron-sized particles act as nucleation sites.
8. The initial adsorption probability amounts to S_0 = 0.92±0.05.

References

1. Ice on the Moon. http://nssdc.gsfc.nasa.gov/planetary/ice/ice_moon.html Accessed July 9, 2008.
2. Feldman, W.C., et al.: Fluxes of Fast and Epithermal Neutrons From Lunar Prospector: Evidence for Water Ice at the Lunar Poles. Science, vol. 281, no. 5382, 1998, pp. 1496−1500.
3. Spudis, P.D.: World Book Online Reference Center. World Book, Inc., 2004. http://www.worldbookonline.com/wb/Article?id=ar37006 Accessed July 9, 2008.
4. Ritterskamp, Peter, et al.: A Titanium Disilicide Derived Semiconducting Catalyst for Water Splitting Under Solar Radiation—Reversible Storage of Oxygen and Hydrogen. Angew. Chem. Int. Ed., vol. 46, no. 41, 2007, pp. 7770−7774.
5. Flavell, W.R., et al.: H_2O Adsorption on $Bi_2Sr_2CaCu_2O_8$(001). Phys. Rev. B, vol. 41, 1990, pp. 11623−11626.
6. Westbrook, J.H.; and Jorgensen, P.J.: Effects of Water Desorption on Indentation Microhardness Anisotropy in Minerals. Amer. Mineral., vol. 53, 1968, p. 1899.
7. Rickman, Doug; and Street, Kenneth W.: Some Expected Mechanical Characterstics of Lunar Dust: A Geological View. AIP Conf. Proc., vol. 969, issue 1, 2008.
8. Molina, M.J., et al.: Antarctic Stratospheric Chemistry of Chlorine Nitrate, Hydrogen Chloride, and Ice: Release of Active Chlorine. Science, vol. 238, no. 4831, 1987, pp. 1253−1257.
9. Astromaterials Curation at NASA JSC. http://curator.jsc.nasa.gov/lunar/index.cfm Accessed July 9, 2008.
10. Taylor, L.A.: 2005 Planetary Geosciences Institute, The University of Tennessee, Knoxville, TN, 2005.
11. Street, K.W., et al.: In preparation.
12. Funk, S., et al.: Adsorption Dynamics of Alkanes on Single-Wall Carbon Nanotubes: A Molecular Beam Scattering Study. J. Phys. Chem. C, vol. 111, 2007, pp. 8043−8049.
13. Thiel, Patricia A.; and Madey, Theodor E.: The Interaction of Water With Solid Surfaces: Fundamental Aspects. Surf. Sci. Rep., vol. 7, 1987, p. 211−385.
14. Henderson, Michael A.: The Interaction of Water With Solid Surfaces: Fundamental Aspects Revisited. Surf. Sci. Rep., vol. 46, 2002, pp. 1−308.
15. Smith, R. Scott; and Kay, Bruce D.: Molecular Beam Studies of Kinetic Processes in Nanoscale Water Films. Surface Review and Letters, vol. 4, issue 4, 1997, pp. 781−797.
16. Kimmel, Greg A., et al.: Control of Amorphous Solid Water Morphology Using Molecular Beams. I. Experimental Results. J. Chem. Phys., vol. 114, no. 12, 2001, pp. 5284−5294.
17. Morgenstern, Markus; Michely, Thomas; and Comsa, George: Anisotropy in the Adsorption of H_2O at Low Coordination Sites on Pt(111). Phys. Rev. Lett., vol. 77, 1996, pp. 703−706.
18. Joly, J.P., et al.: Temperature-Programmed Desorption (TPD) of Water From Iron, Chromium, Nickel and 304 L Stainless Steel. Vacuum, vol. 59, no. 4, 2000, pp. 854−867.
19. Joseph, Y., et al.: Adsorption of Water on FeO(111) and Fe_3O_4(111): Identification of Active Sites for Dissociation. Chem. Phys. Lett., vol. 314, issues 3−4, 1999, pp. 195−202.
20. Daschbach, John L., et al.: Water Adsorption, Desorption, and Clustering on FeO(111). J. Phys. Chem. B, vol. 109, 2005, pp. 10362−10370.
21. Wu, Ming-Cheng, et al.: Model Surface Studies of Metal Oxides: Adsorption of Water and Methanol on Ultrathin M_gO Films on Mo(100). J. Chem. Phys., vol. 96, issue 5, 1992, p. 3892.
22. Wendt, S., et al.: The Interaction of Water With Silica Thin Films Grown on Mo(112). Surf. Sci., vol. 565, 2004, pp. 107−120.
23. Kaya, S., et al.: Formation of an Ordered Ice Layer on a Thin Silica Film. J. Phys. Chem. C, vol. 111, no. 2, 2007, pp. 759−764.
Library unable to verify the following:
24. Kunat, M., et al.: Phys. Chem. Chem. Phys., vol. 6, 2004, p. 4203.

25. Lim, D.S.-W.; and Stuve, E.M.: Solvation and Ionization of Hydroxyl Groups in Water-Ice Layers on Silver (110). Surf. Sci., vol. 425, 1999, pp. 233−244.
26. Liu, Ping, et al.: Reaction of Water With Vacuum-Cleaved CaO(100) Surfaces: An X-Ray Photoemission Spectroscopy Study. Surf. Sci., vol. 416, 1998, pp. 326−340.
27. Willis, R.F., et al.: Photoemission and Secondary Electron Emission From Lunar Surface Material. Astrophysics and Space Science Library, Vol. 37, 1973, pp. 389−401.
28. Wilkinson, A.: NASA Exploration Soil Bibliographic Database. Available to registered users through http://outtek.grc.nasa.gov/Soils-Bib Accessed Dec. 2007
29. Hurowitz, Joel A.; and McLennan, Scott M.: A ~3.5 Ga Record of Water-Limited, Acidic Weathering Conditions on Mars. Earth Planetary Sci. Lett., vol. 260, 2007, pp. 432−443.
30. Hurowitz, Joel A., et al.: Production of Hydrogen Peroxide in Martian and Lunar Soils. Earth Planetary Sci. Lett., vol. 255, 2007, pp. 41−52.
31. Wang, J.; and Burghaus, U.: Adsorption Dynamics of CO_2 on Zn-ZnO(0001): A Molecular Beam Study. J. Chem. Phys., vol. 122, no. 4, 2005, p. 044705.
32. Funk, S.; Nurkic, T.; and Burghaus, U.: Reactivity Screening of Silica. Applied Surface Science, vol. 253, issue 11, 2007, pp. 4860−4865.
33. Smith, R. Scott, et al.: The Self-Diffusivity of Amorphous Solid Water Near 150 K. Chem. Phys., vol. 258, 2000, pp. 291−305.
34. Haq, S.; Harnett, J.; and Hodgson, A.: Growth of Thin Crystalline Ice Films on Pt(111). Surf. Sci., vol. 505, 2002, pp. 171−182.
35. Seets, D.C.; Wheeler, M.C.; and Mullins, C.B.: Mechanism of the Dissociative Chemisorption of Methane Over Ir(110): Trapping-Mediated or Direct? Chem. Phys. Lett., vol. 266, 1997, pp. 431−436.
36. Raschke, Markus B.; and Madey, Theodore E.: Transmission of Low-Energy ($\leq$10 eV) H^+ and D^+ Ions Through Ultrathin Rare-Gas Films. Phys. Rev. B, vol. 58, no. 23, 1998−I, p. 15 832.
37. Funk, S.; Goering, J.; and Burghaus, U.: Adsorption Kinetics and Dynamics of Small Organic Molecules on a Silica Wafer: Butane, Pentane, Nonane, Thiophene, and Methanol Adsorption on SiO_2/Si(111). Applied Surface Science, 2008.
38. Goering, J.; and Burghaus, U.: Adsorption Kinetics of Thiophene on Single-Walled Carbon Nanotubes (CNTs). Chem. Phys. Lett., vol. 447, 2007, pp. 121−126.
39. Zimbitas, G., et al.: Wetting of Mixed OH/H_2O Layers on Pt(111). J. Chem. Phys., vol. 128, no. 7, 2008, p. 074701.

REPORT DOCUMENTATION PAGE

1. REPORT DATE (DD-MM-YYYY) 01-09-2008	2. REPORT TYPE Technical Memorandum	3. DATES COVERED (From - To)

4. TITLE AND SUBTITLE
Adsorption of Water on Simulated Moon Dust Samples

5a. CONTRACT NUMBER

5b. GRANT NUMBER

5c. PROGRAM ELEMENT NUMBER

6. AUTHOR(S)
Goering, John, P.; Sah, Shweta; Burghaus, Uwe; Street, Kenneth, W., Jr.

5d. PROJECT NUMBER

5e. TASK NUMBER

5f. WORK UNIT NUMBER
WBS 936374.03.03.03

7. PERFORMING ORGANIZATION NAME(S) AND ADDRESS(ES)
National Aeronautics and Space Administration
John H. Glenn Research Center at Lewis Field
Cleveland, Ohio 44135-3191

8. PERFORMING ORGANIZATION REPORT NUMBER
E-16559

9. SPONSORING/MONITORING AGENCY NAME(S) AND ADDRESS(ES)
National Aeronautics and Space Administration
Washington, DC 20546-0001

10. SPONSORING/MONITORS ACRONYM(S)
NASA

11. SPONSORING/MONITORING REPORT NUMBER
NASA/TM-2008-215279

12. DISTRIBUTION/AVAILABILITY STATEMENT
Unclassified-Unlimited
Subject Category: 91
Available electronically at http://gltrs.grc.nasa.gov
This publication is available from the NASA Center for AeroSpace Information, 301-621-0390

13. SUPPLEMENTARY NOTES

14. ABSTRACT
A lunar regolith simulant dust sample (JSC-1a) supported on a silica wafer (SiO_2/Si(111)) has been characterized by scanning electron microscopy (SEM), energy dispersive x-ray spectroscopy (EDX), and Auger electron spectroscopy (AES). The adsorption kinetics of water has been studied primarily by thermal desorption spectroscopy (TDS) and also by collecting isothermal adsorption transients. The support has been characterized by water TDS. JSC-1a consists mostly of aluminosilicate glass and other minerals containing Fe, Na, Ca, and Mg. The particle sizes span the range from a few microns up to 100 μm. At small exposures, H_2O TDS is characterized by broad (100 to 450 K) structures; at large exposures distinct TDS peaks emerge that are assigned to amorphous solid water (145 K) and crystalline ice (165 K). Water dissociates on JSC-1a at small exposures but not on the bare silica support. It appears that rather porous condensed ice layers form at large exposures. At thermal impact energies, the initial adsorption probability amounts to 0.92±0.05.

15. SUBJECT TERMS
Absorption; Water; Lunar simulant

16. SECURITY CLASSIFICATION OF:			17. LIMITATION OF ABSTRACT	18. NUMBER OF PAGES	19a. NAME OF RESPONSIBLE PERSON STI Help Desk (email:help@sti.nasa.gov)
a. REPORT U	**b. ABSTRACT** U	**c. THIS PAGE** U	UU	16	**19b. TELEPHONE NUMBER** (include area code) 301-621-0390